

Molecular-dynamics study of oxygen diffusion in $\text{YBa}_2\text{Cu}_3\text{O}_{6.91}$

X. Zhang* and C. R. A. Catlow

Davy Faraday Research Laboratory, The Royal Institution of Great Britain, 21 Albemarle Street, London W1X 4BS, United Kingdom

(Received 18 October 1991; revised manuscript received 27 March 1992)

Oxygen diffusion in $\text{YBa}_2\text{Cu}_3\text{O}_{6.91}$ at high temperatures (1400–1500 K) has been studied with use of molecular-dynamics simulation techniques employing Born model potentials. The oxygen diffusion is found to occur mainly within the Cu(1)-O basal plane by a vacancy mechanism; and the oxygen diffusion coefficient (D) is calculated as $D = 1.4 \times 10^{-4} \exp[(-0.98 \text{ eV}/kT)] \text{ cm}^2 \text{ s}^{-1}$, which is in good agreement with experimental results. Details of the oxygen-migration mechanisms are obtained from particle trajectories which are analyzed with use of molecular-graphics techniques. The oxygen vacancies are found to migrate between O(1), O(4), and O(5) sites, but not to O(2) and O(3) sites. The possible oxygen-ion-jump paths are observed to be O(1)-O(5), O(1)-O(4), and O(4)-O(5).

INTRODUCTION

Diffusion is among the most important solid-state processes and is of great importance in materials processing. High- T_c superconductors are no exception in this respect. The most important and widely studied diffusion phenomenon in $\text{YBa}_2\text{Cu}_3\text{O}_{7-x}$ involves oxygen migration. It is well known that the critical temperature T_c of $\text{YBa}_2\text{Cu}_3\text{O}_{7-x}$ depends on the value of x .¹ To retain a high value of T_c , the material has to be kept as fully oxygenated as possible. To achieve this goal it is necessary to understand the mechanism of diffusion of oxygen and to obtain accurate values of the diffusion coefficient.

The importance of oxygen transport in $\text{YBa}_2\text{Cu}_3\text{O}_{7-x}$ has resulted in a number of studies by a variety of experimental techniques. Xie, Chen, and Wu,² using internal-friction measurements, interpreted their data in terms of diffusional jumps in the basal planes between sites O(5) and O(1) (see Fig. 1) and obtained an activation energy of 1.03 eV. Zhang *et al.*³ reported internal-friction measurements and measured an activation energy of 1.12 eV for the orthorhombic phase. In particular, they proposed

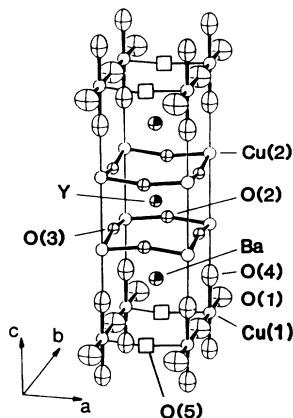


FIG. 1. Structure of $\text{YBa}_2\text{Cu}_3\text{O}_7$.

that oxygen migration is associated with either an ordering diffusion process between layers or an order or disorder diffusion process in the Cu(2) plane. Tu *et al.*⁴ carried out *in situ* resistivity measurements to monitor the variation in oxygen content and reported activation energies of 0.5 eV at $x=0.38$ and of 1.3 eV at $x=0$ in the temperature range of 250–500°C. Carrillo-Cabrera, Wiemhofer, and Gopel⁵ reported ionic conductivity studies and obtained an activation energy of 2.2 eV. They assumed that oxygen migration would mainly occur within the Cu(1) basal plane by a vacancy mechanism. From thermogravimetric studies of chemical diffusion Kishio *et al.*⁶ proposed that oxygen diffusion proceeds via an interstitial-like mechanism in the basal plane and measured an activation energy of 1.38 eV at $x=0$. Rothman *et al.*^{7,8} undertook measurements of oxygen tracer diffusion and indicated that diffusion is highly anisotropic with diffusion in the ab plane being much faster than along the c axis. Furthermore, they concluded that the diffusion coefficient for the faster component may be described by a single activation energy of 0.97 eV over a wide range of stoichiometry. Ottaviani *et al.*⁹ studied oxygen diffusion in tetragonal $\text{YBa}_2\text{Cu}_3\text{O}_{6.35}$ using *in situ* resistivity measurements and suggested an activation energy of 0.40 eV. The activation energies reported by different workers clearly show significant scatter, which may, of course, be partly attributed to differences in experimental conditions.

Oxygen diffusion in $\text{YBa}_2\text{Cu}_3\text{O}_{7-x}$ has also been studied theoretically. Choi *et al.*¹⁰ undertook a calculation of oxygen tracer diffusion coefficients using the cluster variation technique in conjunction with the path probability method and reported activation energies of 0.8 eV and 1.2 eV in the tetragonal and orthorhombic phases, respectively. They also found a stoichiometry-dependent diffusion coefficient and a break in the Arrhenius plot at the orthorhombic-tetragonal transition. Baetzold¹¹ obtained an oxygen-migration energy of 0.3 eV using a shell model and associated two- and three-body short-range interaction potentials. By assuming that the force

between two neighboring oxygen ions was repulsive for an O(1) and O(5) site, repulsive for two O(1) sites in the a direction, and attractive in the b direction, Tu *et al.*⁴ obtained a strong anisotropy of the diffusion coefficient in the ab plane and a strong stoichiometry dependence of the diffusion coefficient. Ronay and Nordlander¹² carried out a mean-field calculation and suggested that oxygen could move interstitially over the O(5) site (along channels parallel to the b direction) with an almost zero activation energy for motion, whereas the activation energies for diffusion in the a and c directions were ~ 1.7 eV. Islam¹³ studied oxygen migration in $\text{YBa}_2\text{Cu}_3\text{O}_7$ using computer simulation techniques. His results support the models in which ionic diffusion is attributed to the mobility of oxygen vacancies and showed that vacancy diffusion via the O(1)-O(4)-O(1) path was energetically the most favorable, with a migration energy of 0.72 eV.

From the range of studies on oxygen diffusion in $\text{YBa}_2\text{Cu}_3\text{O}_{7-x}$ there appears to be general qualitative agreement that diffusion in the ab plane is much faster than in the c direction, but there is not much agreement on the details of the diffusion path or of the activation energies.⁸ The information provided by experimental diffusion studies can only rarely be sufficiently to identify atomic diffusion mechanisms, particularly for complex structures. In addition, static lattice calculations of the type summarized above, although unquestionably useful, are limited in that they can at best explore the energy surfaces for proposed mechanisms rather than reveal the mechanism directly. These limitations are removed by molecular dynamics (MD), which is ideally suited to probing diffusion mechanisms. We have therefore undertaken a molecular-dynamics study of oxygen diffusion in $\text{YBa}_2\text{Cu}_3\text{O}_{6.91}$ at high temperatures (1400–1600 K) in an attempt to investigate the oxygen diffusion mechanism.

METHOD

Molecular dynamics (MD) studies have become a standard tool in computational chemistry, since their introduction in 1957 by Alder and Wainwright.¹⁴ The technique has been applied to a wide range of systems from molten ionic solids to enzyme-substrate interactions and is as noted as ideally suited to investigating diffusion mechanisms. The MD method requires a potential-energy function that provides a rapidly calculable description of the energy and a first derivative vector of the system as a function of its structure. Given the forces provided by this energy function and the known atomic masses, an acceleration vector is readily obtainable for the system. A set of starting velocities (usually randomly assigned) provides a starting point, and the MD method proceeds by solving Newton's equations of motion using a finite time step. This numerical integration procedure yields a new set of atomic coordinates and forces. Repetition of this algorithm yields a detailed picture of the evolution of the system as a function of time. The choice of time step in the integration stage is critical: too small and computer time is wasted; too large and energy is not conserved (the integration is inaccurate).

The accuracy of the simulation as a whole is deter-

mined by the quality of the interatomic potentials describing the system. In deriving potential parameters for ionic material two broad strategies are available: first we can fit variable potential parameters to available crystal properties (such as crystal structure, elastic constant, dielectric constant, etc.); secondly, we attempt to calculate ionic interaction directly by theoretical methods. The first approach is used in this work. Baetzold¹⁵ has developed a set of shell-model potentials that have been successfully used in static simulations of $\text{YBa}_2\text{Cu}_3\text{O}_7$. Because it is extremely expensive in computational terms to use the shell model in MD calculation, we used rigid-ion models in this study as has been the case in most MD studies of solids. We use Born model potentials with short-range terms of the Buckingham form

$$\Phi = A \exp(-r/\rho) - C/r^6. \quad (1)$$

Baetzold's¹⁵ parameters were used as the starting point but were refitted so that the new rigid-ion parameters reproduced the structure of $\text{YBa}_2\text{Cu}_3\text{O}_7$. The model uses formal charge of 3+, 2+, and 2+ for Y, Ba, and Cu, respectively. All O ions, except O(1), were given a charge of 2-; O(1) has a charge of 1-. The potential parameters used in the study are listed in Table I. The potential reproduces the structure of $\text{YBa}_2\text{Cu}_3\text{O}_7$ with a maximum error in any structural parameter of 5% (see Table II).

We used an oxygen composition corresponding to $\text{YBa}_2\text{Cu}_3\text{O}_{6.91}$, which is close to that for which the fastest oxygen diffusion is observed. In order to simulate $\text{YBa}_2\text{Cu}_3\text{O}_{6.91}$, we took three O(1) out of 32 $\text{YBa}_2\text{Cu}_3\text{O}_7$ units (which are comprised of 416 atoms) to create three oxygen vacancies before the start of the simulation, and then assigned three of the O(1) species a charge of 2- in order to retain electroneutrality. The simulations were performed using a (15.22 Å × 15.53 Å × 23.61 Å) box containing 413 atoms. Newton's equations were integrated using the leap-frog algorithm¹⁶ with a 1-ps time step. Initially a Gaussian distribution of velocities was assigned to all the atoms in the simulation box. Iterative velocity scaling was employed to achieve a stable temperature. The system was then allowed to equilibrate for 15 ps prior to production runs for subsequent analysis.

The calculations were performed on the CRAY X-MP supercomputer at Rutherford Appleton Laboratories and the CONVEX C210 computer in our Laboratory using a modified version of the FUNGUS computer code

TABLE I. Potential parameters: Short-range interaction.

	A (eV)	ρ (Å)	C (eV Å ⁶)
$\text{O}^{2-}\text{-O}^{2-}$	22 764.3	0.149 00	25.0
$\text{O}^{2-}\text{-O}^-$	22 764.3	0.149 00	25.0
$\text{O}^{2-}\text{-Cu}^{2+}$	3 799.3	0.242 73	0.0
$\text{O}^{2-}\text{-Ba}^{2+}$	3 115.5	0.335 83	0.0
$\text{O}^{2-}\text{-Y}^{3+}$	20 717.5	0.242 03	0.0
$\text{O}^- \text{-O}^-$	22 764.3	0.149 00	25.0
$\text{O}^- \text{-Cu}^{2+}$	1 861.6	0.252 63	0.0
$\text{O}^- \text{-Ba}^{2+}$	29 906.5	0.272 38	0.0
$\text{Cu}^{2+}\text{-Ba}^{2+}$	168 128.6	0.228 73	0.0
$\text{Ba}^{2+}\text{-Ba}^{2+}$	2 663.7	0.255 80	0.0

TABLE II. Comparison of calculated and experimental bond lengths.

Bond	Calculated length (Å)	Experimental length (Å) ^a	Differences (Å)
Cu(1)-O(1)	1.940	1.940	0.000
Cu(1)-O(4)	1.760	1.847	0.087
Cu(2)-O(2)	1.932	1.925	0.007
Cu(2)-O(3)	1.961	1.957	0.004
Cu(2)-O(4)	2.413	2.299	0.114
Ba-O(1)	3.066	2.964	0.102
Ba-O(2)	2.841	2.944	0.103
Ba-O(3)	2.809	2.883	0.074
Ba-O(4)	2.796	2.740	0.056
Y-O(2)	2.365	2.407	0.042
Y-O(3)	2.348	2.381	0.033

^aReference 20.

developed by Walker.¹⁷ We have made considerable use of molecular-graphics techniques in the analysis of MD trajectories. The molecular modeling package¹⁸ INSIGHT II on a Silicon Graphics workstation was used to animate the framework trajectories for investigating oxygen diffusion mechanism.

RESULTS

Since the primary aim of this work is the investigation of oxygen-diffusion mechanisms, we undertook MD calculation at high temperatures (1400–1500 K). This is in order to ensure that a sufficient number of migration events is recorded during the simulation. Simulation of 100 ps were undertaken in order to obtain sufficient trajectories to investigate in detail the migration mechanisms. Calculation of the mean-square displacement (MSD) of atoms as a function of time leads to a direct measure of the self-diffusion coefficient D via the following equation:¹⁹

$$\langle |r(t) - r(0)|^2 \rangle = B + 6Dt, \quad (2)$$

where $|r(t) - r(0)|$ is the displacement of a particle from its initial position; the brackets denote an average over the particles concerned and over time origins and B is a thermal factor arising from atomic vibrations. Figure 2 shows the MSD plot for the oxygen-ion simulation at 1500 K. It is seen that oxygen diffuses in three directions. The oxygen-diffusion coefficients at different temperatures are calculated from the MSD plots and are given in Table III. We found that the coefficients for oxygen diffusion in the a and b direction are similar and

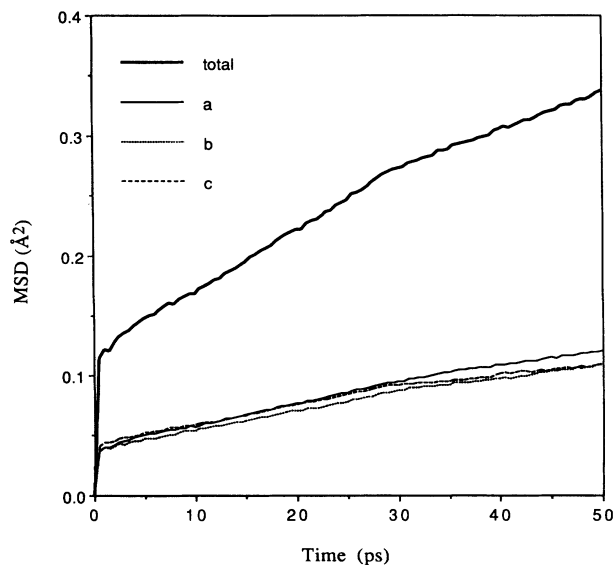


FIG. 2. MSD plot for oxygen migration at 1500 K. Curves a , b , and c correspond to the MSD in the a , b , and c direction, respectively. Curve total corresponds to the total MSD.

they are both larger than the diffusion in the c direction. Because it is difficult to find the experimental diffusion coefficients for oxygen diffusion at high temperatures, we calculated the diffusion coefficients from the expression

$$D = 1.4 \times 10^{-4} \exp[(-0.97 \text{ eV})/kT] \text{ cm}^2 \text{ s}^{-1}, \quad (3)$$

which derives from the experimental data of Rothman, Routbort, and Baker.⁷ The comparison of calculated and experimental diffusion coefficients is reported in Table IV. We found that the calculated diffusion coefficients at 1400 and 1500 K are in good agreement with the (extrapolated) experimental data. The calculated diffusion coefficient at 1450 K is in reasonable but less close agreement with the experimental value because it was obtained from the production run of 60 ps, whereas the other two data were obtained from a production run of 100 ps. We used the production run of 60 ps at 1450 K because after 60 ps the MSD curve showed anomalous behavior, with the vacancies becoming “locked” into an immobile configuration. Such eventualities are a hazard when simulating systems with relatively low diffusion coefficients. Because the calculated data for oxygen diffusion at 1400 and 1500 K are most accurate, we base our Arrhenius plot [$\ln(D)$ vs T^{-1}] (Fig. 3), we obtained an

TABLE III. Calculated diffusion coefficients.

T (K)	D ($10^{-8} \text{ cm}^2 \text{ s}^{-1}$)	D_a ($10^{-8} \text{ cm}^2 \text{ s}^{-1}$)	D_b ($10^{-8} \text{ cm}^2 \text{ s}^{-1}$)	D_c ($10^{-8} \text{ cm}^2 \text{ s}^{-1}$)
1400	4.5 ± 0.2	1.82 ± 0.03	1.70 ± 0.02	0.96 ± 0.03
1450	5.6 ± 0.6	2.23 ± 0.07	2.10 ± 0.07	1.54 ± 0.07
1500	7.6 ± 0.3	2.83 ± 0.03	2.47 ± 0.04	2.35 ± 0.05

TABLE IV. Comparison of calculated diffusion coefficients and experimental diffusion coefficients.

T (K)	Experimental D^a (10^{-8} cm 2 s $^{-1}$)	Calculated D (10^{-8} cm 2 s $^{-1}$)
1400	4.53	4.5 ± 0.2
1450	5.97	5.6 ± 0.6
1500	7.74	7.6 ± 0.3

^aCalculated from the diffusion coefficient expression of $D = 1.4 \times 10^{-4} \exp[(-0.97 \text{ eV}/kT)]$ (cm 2 s $^{-1}$) (Ref. 7).

activation energy of 0.98 eV with $D_0 = 1.4 \times 10^{-4}$ cm 2 s $^{-1}$.

Rothman, Routbort, and Baker,⁷ whose sample had a similar oxygen stoichiometry to that used in our simulation, reported the oxygen tracer diffusion coefficient of $\text{YBa}_2\text{Cu}_3\text{O}_{7-x}$ as

$$D = 1.4 \times 10^{-4} \exp[(-0.97 \text{ eV})/kT] \text{ cm}^2\text{s}^{-1}. \quad (4)$$

Our calculated oxygen-diffusion coefficient, which can be expressed as

$$D = 1.4 \times 10^{-4} \exp[(-0.98 \text{ eV})/kT] \text{ cm}^2\text{s}^{-1}, \quad (5)$$

is in very good agreement with the result of Rothman, Routbort, and Baker⁷ and is also close to the result of Xie, Chen, and Wu:²

$$D = 3.5 \times 10^{-4} \exp[(-1.03 \text{ eV})/kT] \text{ cm}^2\text{s}^{-1}. \quad (6)$$

We should stress, however, that the very accurate numerical agreement between theoretical and experimental values of D_0 and activation energy is fortuitous in view of the small number of simulated data points.

An advantage of using MD is that the diffusion mechanism can be viewed directly by analysis of MD particle trajectories. We have therefore made considerable use of molecular graphics techniques in the analysis of oxygen trajectories. As noted, we started the calculations by putting all the vacancies on O(1) sites. During the simulation we found that oxygen vacancies can migrate between O(1), O(4), and O(5) sites but not to O(2) or O(3) sites [this was also the case when we started the calculations by put-

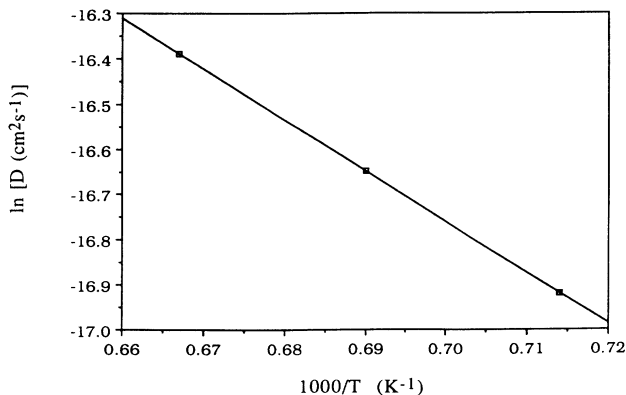


FIG. 3. Calculated Arrhenius plot for oxygen diffusion in $\text{YBa}_2\text{Cu}_3\text{O}_{6.91}$.

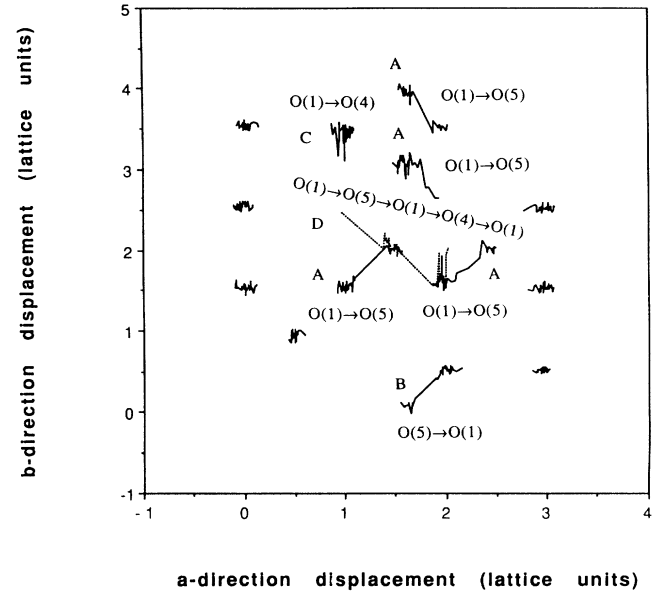


FIG. 4. The xy projection of the coordinates of the oxygen ions situated in the Cu(1)-O plane at 1500 K for a duration of 100 ps. The jump paths for the oxygen ions are ion A: O(1)-O(5); ion B: O(5)-O(1); ion C: O(1)-O(4); and ion D: O(1)-O(5)-O(1)-O(4)-O(1).

ting the vacancies on both O(1) and O(2) sites]. We expect that at lower temperatures there will be no (or very few) vacancies on O(2) and O(3) sites either as implied by the experimental result $D_c \ll D_{ab}$ (see Ref. 7).

Figure 4 shows the xy projection of the coordinates of the oxygen ions situated in the Cu(1)-O plane at 1500 K for a duration of 100 ps. Of the 14 oxygen ions situated

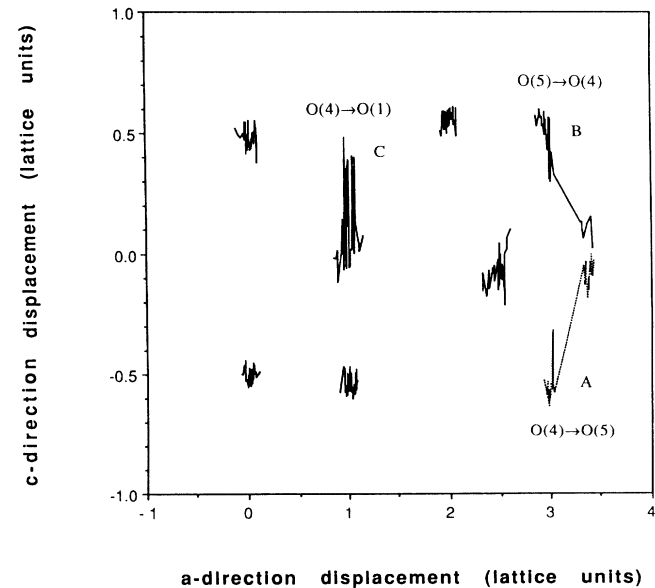


FIG. 5. The xz projection of O(4) coordinates at 1500 K for a duration of 100 ps. The jump paths of the oxygen ions are ion A: O(4)-O(5); ion B: O(5)-O(4); and ion C: O(4)-O(1).

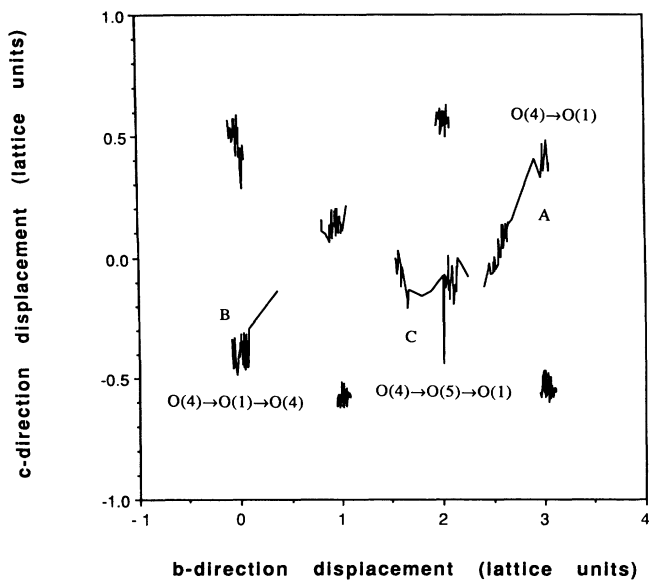


FIG. 6. The yz projection of O(4) coordinates at 1500 K for a duration of 100 ps. The jump paths of the oxygen ions are ion A: O(4)-O(1); ion B: O(4)-O(1)-O(4); and ion C: O(4)-O(5)-O(1).

in this plane, 12 are situated on O(1) sites and the others are situated on O(5) sites at $t = 0$. In the simulation, some of oxygen ions jump into other sites. The jump paths for these oxygen ions are ion A: O(1)-O(5); ion B: O(5)-O(1); ion C: O(1)-O(4); ion D: O(1)-O(5)-O(1)-O(4)-O(1). The rest of the oxygen ions vibrate at their equilibrium sites. Neither O(5)-O(5) nor O(1)-O(1) jumps are observed in this simulation. Jumps of oxygen ions from one O(1) site to another O(1) site appear to take place via an O(5) site (see oxygen-ion D in Fig. 4). We expect that jumps of oxygen ions from one O(5) site to another O(5) site will also occur via O(1) sites.

Figure 5 and 6 show the xz projection and yz projection of O(4) coordinates for a duration of 100 ps (simulated at 1500 K). We observed in Fig. 5 that oxygen ion A jumps from the O(4) site onto the O(5) site. The jump path of oxygen ion A in Figure 5 is O(4)-O(5), the jump path of oxygen ion B is O(5)-O(4), and the jump path of oxygen ion C is O(4)-O(1). From Fig. 6 we observe that oxygen ion A jumps from the O(4) site onto the O(1) site; oxygen ion B jumps from the O(4) site onto the O(5) site and then jumps back onto the O(4) site; the jump path of oxygen ion C is more complex: it jumps first from the O(4) site onto the O(5) site and then jumps onto the O(1) site. Most O(4) ions vibrate around their equilibrium sites. Jumps of the type O(4)-O(2), O(4)-O(3), or O(4)-O(4) are not observed in this simulation.

Thus to summarize our analysis of the oxygen trajectories using molecular graphics techniques, we have found that jumps in the ab plane are more frequent than those in the c direction. The possible oxygen-ion jump paths we found are O(1)-O(5), O(1)-O(4), and O(4)-O(5).

DISCUSSION

As noted, our model assumes a charge of -1 for oxygen on the O(1) site but -2 on the other sites. This im-

plies that if an oxygen ion moves from or to an O(1) site it must continuously change its charge in the process. Actually we found that when the system reaches equilibrium most of oxygen ions with charge -1 go to the O(2) and O(3) sites. Some O^- ions move to the O(4) sites and only a very small proportion of them still remain in the O(1) sites. We noted no movement of oxygen ions at the O(2) and O(3) sites, and a only very rare movement of O^- ions at the O(1) and O(4) sites. This suggests that the mobile oxygen ions in $YBa_2Cu_3O_{6.91}$ are O^{2-} .

Rothman *et al.*⁸ found that the diffusion coefficient in the b direction D_b is much larger than that in the a direction D_a at 300°C and that a linear Arrhenius plot is observed over the entire temperature range. Combining these results, they suggest that the condition $D_b \gg D_a$ should hold over the entire temperature range. Our results do not agree with this aspect of their work, as we find that $D_a \sim D_b$ in the temperature range of 1400–1500 K.

We noted that there are oxygen-ion jumps from O(1) or O(5) sites to O(4) sites but no jumps from O(2) or O(3) sites to O(4) sites. This may be related to the fact that the O(2) [O(3)]-O(4) distance of ~ 3.0 Å is much greater than the O(1) [O(5)]-O(4) distance of ~ 2.5 Å. The migration energy for moving an oxygen ion from an O(2) or O(3) site to an O(4) site is expected to be much larger than that for moving an oxygen ion from the O(1) or O(5) site to the O(4) site.

We also note in Fig. 2 and Table III that D_c is smaller than D_a and D_b but is apparently nonzero. Our graphic analysis has already shown that there is no jump of O(4)-O(2) or O(4)-O(3). To what, therefore, can we attribute this nonzero value of D_c ? It appears that this is due to the jumps of O(1)-O(4) and O(5)-O(4). We should also recall that our MD simulation samples only 100 ps of real time. Our oxygen-ion trajectories (Figs. 4–6) show that in this time the oxygen ions jump only 2–3 times. These time scales are too short for us to obtain meaningful quantitative results for diffusion parallel to the c direction, although it is clear that this is very small compared to diffusion in a and b directions; i.e., $D_c \ll D_{ab}$, as found experimentally.

From the analyses of their experimental data, which, as noted, give $D_b \gg D_a$, and $D_{ab} > 10^4 - 10^6 \times D_c$, Rothman *et al.*⁸ proposed an oxygen-diffusion mechanism for $YBa_2Cu_3O_{7-x}$. They suggested that an oxygen ion at the end of a row of O(1) sites jumps onto an O(5) site, moves along the O(5) site until it comes to another row end, and attaches itself. Islam¹³ regarded the oxygen migration along O(5) sites in orthorhombic $YBa_2Cu_3O_{7-x}$ as oxygen interstitial migration. His calculation showed that such a mechanism needs an activation energy of 3.5 eV, which is much larger than the migration energy needed for moving an oxygen ion along the O(1)-O(4) path (0.5–0.7 eV). Islam's results contradict calculations of Ronay and Nordlander¹⁴ that a near-zero activation energy is needed for moving oxygen ions along O(5) sites. In agreement with Islam, we did not observe oxygen ions moving along O(5) sites in our MD simulation. We found that the oxygen ion on the O(5) site can easily jump onto

an O(1) site. Of course our results are obtained at high simulated temperatures rather than at the lower temperatures at which most experimental oxygen-diffusion studies were carried out. But it seems implausible that there would be very major changes in the energetics of migration with temperature. As an alternative, might we propose that oxygen ions move along the path O(1)-O(5)-O(1)? If this occurs at lower temperatures, then D_a will be close to D_b , which does not agree with the experimental observation $D_b \gg D_a$.

To reconcile these difficulties we propose the following oxygen diffusion mechanism in $\text{YBa}_2\text{Cu}_3\text{O}_{7-x}$: at lower temperatures, because of the low occupancy of the O(5) site, oxygen vacancy jumps of the type O(1)-O(4)-O(1) will predominate. Such a mechanism does not effect diffusion along the a axis; therefore such a process alone would lead to $D_a = 0$ and $D_b > 0$. However, some O(1)-O(5)-O(1) jumps will occur, but they should be comparatively rare, leading to $D_b \gg D_a$. We recall that there are very few vacancies on O(2) and O(3) sites; oxygen jumps in the c direction will be very restricted leading to $D_{ab} \gg D_c$. These mechanisms seem able to explain the oxygen diffusion behavior at lower temperatures (i.e., $D_b \gg D_a$ and $D_{ab} \gg D_c$) without invoking O(5)-O(5) jumps. These mechanisms also agree with the results of oxygen isotope experiments that both O(1) and O(4) sites are involved in the diffusion mechanism.²¹ At higher temperatures the O(5) site is more easily occupied so that jumps from the O(1) site to the O(5) site begin to occur with the frequency of those jumps from the O(1) site to the O(4) site as our MD result revealed. In this case the oxygen diffusion will mainly be via the ab plane rather than via the chain along b direction. This will result in $D_a \sim D_b$ and $D_{ab} > D_c$ as our simulation result revealed.

Because our MD simulation can only detect the diffusion coefficients larger than $\sim 1 \times 10^{-8} \text{ cm}^2 \text{ s}^{-1}$ us-

ing the simulation times in the present study, it is very difficult for us to carry out MD simulations in the temperature range of 300–700 °C, where most experimental studies of oxygen diffusion in $\text{YBa}_2\text{Cu}_3\text{O}_{7-x}$ are undertaken. Simulation of lower temperature systems are probably best carried out using static methods, which may be used to investigate the energetics of the mechanisms revealed by the dynamics simulations.

CONCLUSIONS

MD simulation of oxygen diffusion in $\text{YBa}_2\text{Cu}_3\text{O}_{6.91}$ in the temperature range 1400–1500 K yield an oxygen-diffusion coefficient of $D = 1.4 \times 10^{-4} \exp[(-0.98 \text{ eV})/kT] \text{ cm}^2 \text{ s}^{-1}$, which is in good agreement with experiment data from lower temperature studies. Oxygen jump paths were also investigated using molecular graphics techniques. We found that oxygen vacancies migrate between O(1), O(5), and O(4) sites but not to O(2) and O(3) sites. The possible oxygen-ion jump paths observed are O(1)-O(5), O(1)-O(4), and O(4)-O(5), but not O(5)-O(5). On the basis of these data, we propose that oxygen diffusion in $\text{YBa}_2\text{Cu}_3\text{O}_{6.91}$ does not take place by the movement of oxygen ions over O(5) sites between the rows of oxygen ions but rather by the movement of oxygen ions along the path O(1)-O(4)-O(1) at lower temperatures and by the movement of oxygen ions mainly along the path O(1)-O(5)-O(1) at higher temperatures.

ACKNOWLEDGMENTS

The authors are grateful to B. Vessal, M. Kawano, G. Sesé, and E. Hernandez for their help with the MD simulations. Useful discussions with S. Islam and R. Baetzold are also gratefully acknowledged. We would like to thank SERC for a research grant.

*Present address: Department of Physics, National University of Singapore, Blk. S12, Lower Kent Ridge Road, Singapore 0511.

¹J. D. Jorgensen, H. Shaked, D. G. Hinks, B. Dabrowski, B. W. Veal, A. P. Paulikas, L. J. Nowicki, G. W. Crabtree, W. L. Kwok, L. H. Nunez, and H. Claus, *Physica C* **153-155**, 578 (1988).

²X. M. Xie, T. G. Chen, and Z. L. Wu, *Phys. Rev. B* **40**, 4549 (1989).

³J. X. Zhang, G. M. Lin, W. G. Zeng, K. F. Liang, Z. C. Lin, G. G. Sin, M. J. Stokes, and P. C. W. Fung, *Supercond. Sci. Technol.* **3**, 113 (1990).

⁴K. N. Tu, N. C. Yeh, S. I. Park, and C. C. Tsuei, *Phys. Rev. B* **39**, 304 (1989).

⁵W. Carrillo-Cabrera, H.-D. Wiemhofer, and W. Gopel, *Solid State Ionics* **32/33**, 1172 (1989).

⁶K. Kishio, K. Suzuki, T. Hasegawa, T. Yamanoto, K. Kitazawa, and K. Fwaki, *J. Solid State Chem.* **82**, 192 (1989).

⁷S. J. Rothman, J. L. Routbort, and J. E. Barker, *Phys. Rev. B* **40**, 8852 (1989).

⁸S. J. Rothman, J. L. Routbort, U. Welp, and J. E. Baker, *Phys. Rev. B* **44**, 2326 (1991).

⁹G. Ottaviani, C. Nobih, F. Nava, M. Affronte, T. Manfredini, F. C. Maticotta, and E. Galli, *Phys. Rev. B* **39**, 9069 (1989).

¹⁰J.-S. Choi, M. Sarikaya, I. A. Aksay, and R. Kikuchi, *Phys. Rev. B* **42**, 4244 (1990).

¹¹R. C. Baetzold, *Phys. Rev. B* **42**, 56 (1990).

¹²R. Ronay and P. Nordlander, *Physica C* **153-155**, 834 (1988).

¹³M. S. Islam, *Supercond. Sci. Technol.* **3**, 531 (1990).

¹⁴B. J. Alder and T. E. Wainwright, *J. Chem. Phys.* **27**, 1208 (1957).

¹⁵R. C. Baetzold, *Phys. Rev. B* **38**, 11 304 (1988).

¹⁶O. J. Buneman, *Comp. Phys.* **1**, 517 (1967).

¹⁷J. R. Walker, in *Computer Simulation of Solids*, edited by C. R. A. Catlow and W. C. Mackrodt, Lecture Notes in Physics, Vol. 166 (Springer, Berlin, 1982), Chap. 5.

¹⁸INSIGHT II, BIOSYM Technologies, Inc., 10065 Barnes Canyon Road, Suite A, San Diego, CA 92121.

¹⁹M. J. Gillan, *Physica* **131B**, 157 (1985).

²⁰F. Beech, S. Miraglia, A. Santoro, and R. S. Roth, *Phys. Rev. B* **35**, 8778 (1987).

²¹W. K. Ham, S. W. Keller, J. N. Michaels, A. M. Stacy, D. Krillov, D. T. Hodul, and R. H. Fleming, *J. Mater. Res.* **4**, 504 (1989).